Supplementary information

1: Relationship between labeling density and the clustering-dependence of FRET

Because FRET intensity depends to the inverse 6th power of the distance between donor and acceptor fluorophore (here GFP-PH-PH and RFP-PH-PH), energy transfer between the PIP_2 probes is a function of both label density and clustering. To estimate the concentration range in which FRET is sensitive for clustering, we calculated dependency of FRET efficiency on both labeling density (D; in molecules per μm^2) and clustering by Monte Carlo simulations using a custom-made Visual Basic program. Briefly, simulations include the following steps.

[1] First, within a (virtual) flat area A of membrane, N donors and N acceptors are positioned randomly or, alternatively, clustered randomly within small circular subdomains of the membrane area. Number and size of subdomains can be varied. At the onset of each simulation, a fraction (typically ≤ 10%) of the donors is excited.

[2] Then, for each excited donor, the chance of energy transfer to any of the acceptors is calculated as follows:

(a) distances of that donor to each of the acceptors are determined and sorted in increasing order $d_1....d_N$;

(b) the theoretical FRET efficiency corresponding to those distances E_d is calculated according to

$$E_d = \frac{R_0^6}{R_0^6 + d^6}$$

Where R_0 = 5 nm (Patterson *et al.*, 2000).

(c) Energy transfer to the nearest acceptor is defined to occur when a computer-generated random number r ($0 \le r \le 1$) is less than or equal to E_{d1}. When there is no FRET, the procedure is repeated for the next-nearest acceptor (E_{d2}), etcetera, until the chance of transfer is negligible ($< 10^{-4}$), in which case the donor does transfer energy to any acceptor.

[3] Upon completion of these calculations for all donor-acceptor pairs, the FRET efficiency E* (percentage of excited donor molecules that transfer their energy) is calculated.

Steps [1]-[3] were carried out for a wide range of densities ($5 \le D \le 125{,}000$) and for various conditions of clustering, including different area% (defined as % of total membrane area that is in clusters), various cluster sizes, and variations in the fraction of fluorophores that locate to the clusters. For any condition, simulations were repeated for at least 5 x 10^5 donors, and the results were averaged. The resulting calculated FRET efficiencies were plotted versus probe density at the membrane.

Using confocal imaging and whole-cell patch clamping, we estimated that our cells have an average volume and membrane area of 1.3 pl and 1100 μm^2, respectively. For GFP constructs containing a single pleckstrin homology domain, which locate for ~50% at the membrane, we previously reported expression levels up to 12 μM (van der Wal *et al.*,

2001) in N1E-115 neuroblastoma cells. Occasionally, cells expressing up to 30 μM where observed. In the HEK293 cells used in this study, expression levels of each of the fluorescently tagged tandem-PH constructs were generally below ~2.5 μM. These chimeras localize exclusively to the plasma membrane, and thus the cellular concentration *C* is related to the average membrane density *D* as:

$$D = C \times 6 \times 10^{23} \times 1.3 \times 10^{-12} / 1100 = C \times 7.1 \times 10^{8} \text{ (molecules / } \mu m^2)$$

The results are depicted in ***Supplementary Figure 1***. Initially, we determined E* for the random situation (***A, left panel, black line***). The simulation predicts ~100% energy transfer at $4x10^4$ molecules/μm^2. This corresponds to a concentration of ~56 μM for each of the constructs; expression levels this high are normally not observed in mammalian cells. Half-maximal FRET occurs at $8x10^3$ molecules/μm^2, and some transfer should be detectable as low as $3x10^2$ molecules/μm^2 (2% FRET). The simulation is in good agreement with experimental data, as we found on average 35% FRET at 10 μM, and up to 70% FRET in cells that were cotransfected with PIP-5-kinase α, which prevented detrimental effects on the cells when the FRET probes were expressed at very high levels. This graph further depicts the simulation results for localization of the fluorophores in a single domain that covers various percentages of the total area (area%), as indicated. Decreasing the area% causes the curves to progressively shift left by up to 20-fold. The maximal decrease in FRET that can be obtained by complete disruption of clusters is found by subtracting these curves from the random, non-clustered case (***middle panel***). From this graph, it is deduced that large FRET changes can be expected even if clusters make up 50% of the membrane area. At a fixed label concentration, the degree of FRET loss is seen to decrease for increasing area% of the clusters (***right panel***).

In ***Figure 1B, left panel***, the effects of different cluster sizes are compared for a fixed area% = 12.5%. It is found that deviations from the random situation are maximal at large cluster sizes (> 6 nm). Nevertheless, even at very small cluster sizes (i.e. 5 nm, as proposed in a recent study (Sharma *et al.*, 2004), substantial loss of FRET should result from cluster disruption (***middle and right panels***).

Figure 1C depicts the results from mixed-population simulations where labels are present in clusters as well as in the rest of the membrane. In mixed populations, the relationship between expression level and FRET efficiency is distinctly biphasic, with the initial, rapid rise at low levels reflecting FRET in clusters, whereas the second more moderate rise represents the remaining membrane area. In these simulations, the space occupied by clusters was kept constant (area% = 10%) and various enrichments within the clusters were modeled at a fixed total numbers of fluorophores. For increasing enrichment in the clusters, we see a progressive shift to the left within the clusters.

As it was described for glycosylphosphatidylinositol-anchored proteins that only 20%-40% of total proteins resided in very small domains (5 nm, Sharma *et al.*, 2004) we also tested what proportion of the total PIP_2 pool could be clustered without being detected by the FRET assay. In ***Figure 1D***, results are summarized for simulations of such small clusters, enriched 3-fold in PIP_2 and containing various fractions of the total PIP_2 pool. It is seen that partitioning of only 2-4% of total PIP_2 in such clusters should result in detectable FRET.

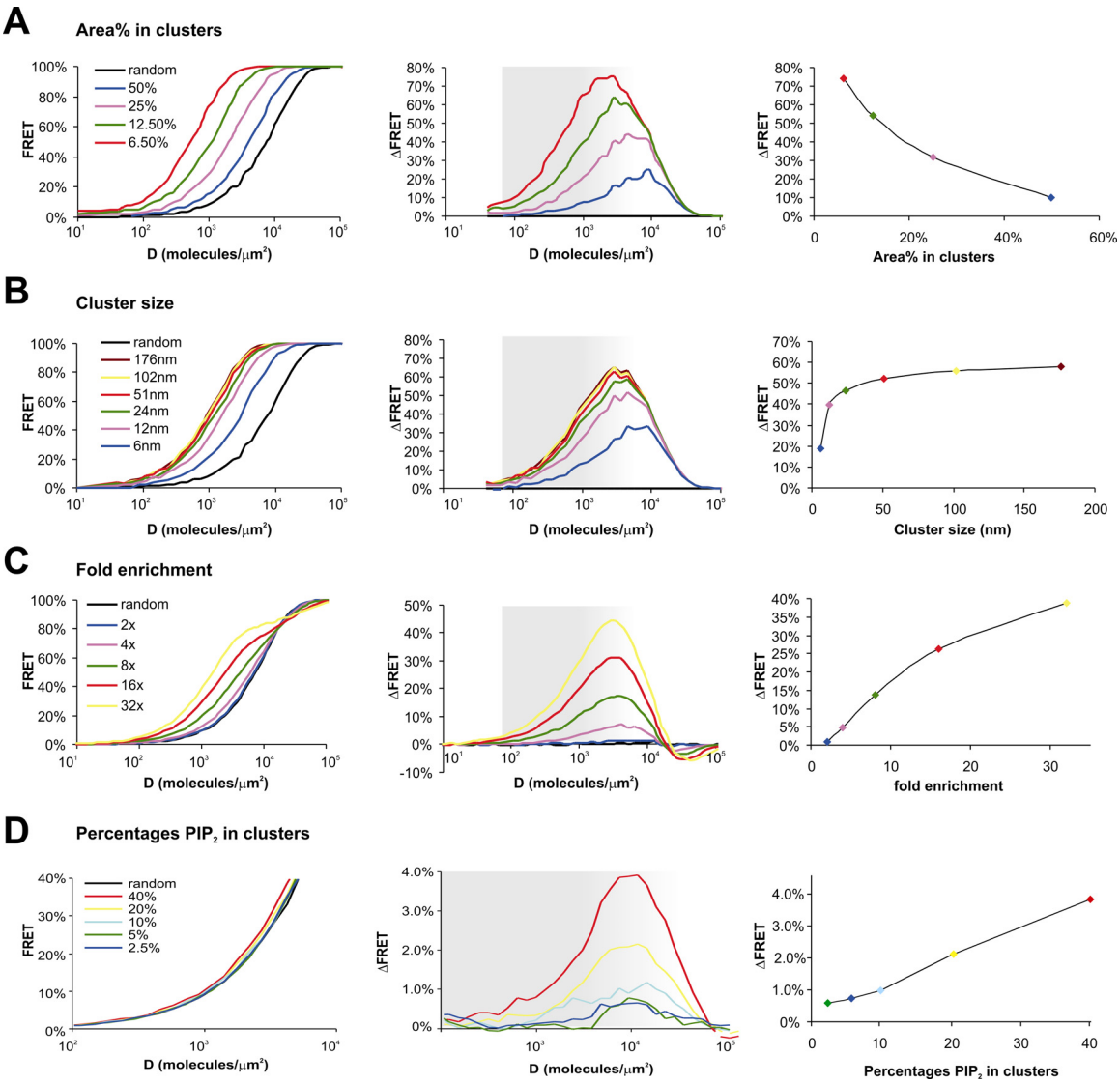

Supplementary Figure 1 FRET dependency on fluorophore density and clustering. (**A**) Fluorophores are present in clusters that constitute the indicated percentage of the total membrane area. (**B**) Effect of cluster size on FRET for fixed area% = 12.5. Note that down to 12 nm, cluster size has little influence on FRET efficiency. (**C**) Monte Carlo simulations for area% = 10 with indicated enrichments of labeling in the domains. (**D**) Monte Carlo simulations for very small cluster sizes (5 nm), enriched 3-fold in PIP_2, and containing the indicated fraction of total PIP_2. Grayed regions in the middle panels indicate densities observed in the experiments. For further details, see the text.

From simulations such as those presented in Figure 1, it is evident that for a wide variety of clustering conditions, micro domain disruption must cause significant loss of FRET at expression levels detected in our cells (0.1-2.5 μM). For example, from Figure 1C it is deduced that enrichment of only 4-fold in clusters that make up 10% of the membrane will give rise to easily detectable (~ 5%) FRET changes at physiological expression levels. Thus, PIP_2 enrichments of 10- to 20-fold, as proposed by Hope and Pike (Hope and Pike, 1996) based on detergent-dependent methods, should be readily detectable.
We conclude that the lack of effect of CD treatment on FRET efficiency observed in large populations of cells can only be interpreted to indicate that PIP_2 is not clustered in these cells.

2: Optimizing assessment of clustering by FRET: experimental details
For all clustering experiments, monomeric eGFP (A206K) and monomeric RFP (Campbell *et al.*, 2002) were used as tags to avoid possible problems due to inherent dimerization of the fluorescent proteins (Zacharias *et al.*, 2002).
In line with reported results (Kenworthy and Edidin, 1998;Zacharias *et al.*, 2002;Glebov and Nichols, 2004), our initial experiments showed considerable cell-to-cell variation in detected FRET values. The reproducibility was enhanced by using constructs with tandem-repeats of the PH domain (see M&M), which causes complete membrane localization. This makes the assay immune to small changes in $[PIP_2]$ that may result from CD treatment (Kwik *et al.*, 2003), thus assuring that any observed differences in FRET reflect distribution of the constructs along the plasma membrane rather than a variable degree of membrane localization. It also avoids bias originating from free 'non-fretting' fluorophores in the cytosol.
Variability was also considerably reduced by collecting paired observations, i.e. by comparing values pre- and post disruption of rafts from the same cells. Analysis of clustering by FRET requires quantitative measurements, and therefore FRET was previously determined by the acceptor photobleaching method (Kenworthy and Edidin, 1998;Zacharias *et al.*, 2002;Glebov and Nichols, 2004). However, this destructive technique is incompatible with paired observations. Therefore, in this study FRET was detected by donor fluorescence lifetime measurements (FLIM). Using a very stable FLIM setup with <1% instrumental drift over several hours allowed reliable detection of population FRET changes considerably less than 1%.
To use a second, independent technique, experiments were also repeated using FRET ratiometry (see M&M). This approach, though not very quantitative, is extremely sensitive to changes from baseline and offers high temporal resolution.

References

Campbell,R.E., Tour,O., Palmer,A.E., Steinbach,P.A., Baird,G.S., Zacharias,D.A. and Tsien,R.Y. (2002) A monomeric red fluorescent protein. *Proc Natl Acad Sci U S A*, **99**, 7877-7882.

Glebov,O.O. and Nichols,B.J. (2004) Lipid raft proteins have a random distribution during localized activation of the T-cell receptor. *Nat. Cell Biol.*, **6**, 238-243.

Hope,H.R. and Pike,L.J. (1996) Phosphoinositides and phosphoinositide-utilizing enzymes in detergent-insoluble lipid domains. *Mol. Biol. Cell*, **7**, 843-851.

Kenworthy,A.K. and Edidin,M. (1998) Distribution of a glycosylphosphatidylinositol-anchored protein at the apical surface of MDCK cells examined at a resolution of <100 A using imaging fluorescence resonance energy transfer. *J. Cell Biol.*, **142**, 69-84.

Kwik,J., Boyle,S., Fooksman,D., Margolis,L., Sheetz,M.P. and Edidin,M. (2003) Membrane cholesterol, lateral mobility, and the phosphatidylinositol 4,5-bisphosphate-dependent organization of cell actin. *Proc. Natl. Acad. Sci. U. S. A*, **100**, 13964-13969.

Patterson,G.H., Piston,D.W. and Barisas,B.G. (2000) Forster distances between green fluorescent protein pairs. *Anal Biochem*, **284**, 438-440.

Sharma,P., Varma,R., Sarasij,R.C., Ira, Gousset,K., Krishnamoorthy,G., Rao,M. and Mayor,S. (2004) Nanoscale organization of multiple GPI-anchored proteins in living cell membranes. *Cell*, **116**, 577-589.

van der Wal,J., Habets,R., Varnai,P., Balla,T. and Jalink,K. (2001) Monitoring agonist-induced phospholipase C activation in live cells by fluorescence resonance energy transfer. *J. Biol. Chem.*, **276**, 15337-15344.

Zacharias,D.A., Violin,J.D., Newton,A.C. and Tsien,R.Y. (2002) Partitioning of lipid-modified monomeric GFPs into membrane microdomains of live cells. *Science*, **296**, 913-916.